Optimization of FFU synthetic sleeper shape in terms of ballast lateral resistance

G.Q. Jing, L. Zong, Y. Ji, and P. Aela*

School of Civil Engineering, Beijing Jiaotong University, Beijing 100044, China.

Abstract. Fiber-reinforced Foamed Urethane (FFU) synthetic sleeper is used in ballasted track with the potential problem of insufficient lateral resistance due to lower weight and smooth surface compared with concrete sleepers. In this paper, the lateral resistance of prototype and modified FFU synthetic sleepers was investigated by single tie push tests and Discrete Element Method (DEM) analysis, where the real shape of ballast particles was created using the 3D scanning technique. Results indicate that due to the smooth surface of sleeper facets, the lateral resistance of prototype FFU sleepers is reduced by 10–15% and governed by the interactions of shoulder ballast and sleeper ends. On the other hand, modification of the sleeper shape by adding FFU strip block along sleeper base and sides increased lateral resistance up to 19% of prototype sleepers with higher interlocking ability between ballast and sleeper sides. Results could be used to develop modified FFU sleepers for application in various ballasted tracks.

1. Introduction

The selection of sleeper type is a key issue in the lateral stability of ballasted railway tracks. Timber sleeper is one of the most common types of sleepers widely used in ballast railway tracks due to the adaptability to be fitted with all types of railway tracks, proper electric insulation, and damping of vibration [1]. However, fungal decay, end splitting, and corrosion are the main causes of failure of timber sleepers, as shown in Figure 1(a) and (b) [2]. In addition, the lateral resistance of timber sleepers was minimum in comparison with other types of sleepers [3,4]. Previous studies confirmed that different types of concrete sleepers have higher lateral resistance due to the high weight and rough surface of

*. *Corresponding author.*
E-mail addresses: gqjing@bjtu.edu.cn (G.Q. Jing);
19121223@bjtu.edu.cn (L. Zong); 17121199@bjtu.edu.cn (Y. Ji); 17119002@bjtu.edu.cn (P. Aela)

sleeper facets [5,6]. Nevertheless, center-bound damage, cracks, and deterioration of rail-seats are the major problems of concrete sleepers (Figure 1(c) and (d)) [2].

Recently, there has been an increasing tendency for the application of composite sleepers as the substitution of existent alternatives due to the high strength to weight ratio, eco-friendly material, and thermal and electrical-insulating properties [7,8]. Despite all advantages, the high cost of manufacturing is the main challenge of using composite sleepers in railway tracks [9]. Generally, composite sleepers are divided into two groups of Engineered Polymer Composite (EPC) and Engineered Wood Product (EWP) [10]. Fiber-reinforced Foamed Urethane (FFU) is a type of EPC sleeper manufactured by Pultrusion. As depicted in Figure 2(a), after mixing glass fibers with polyurethane, the linkage is hardened at a high temperature to provide high strength FFU products. Different shapes of FFU sleepers can be produced, as shown in Figure 2(b). Currently, FFU sleepers have been widely installed in many countries with an expected service life of more than 50 years [11,12] (Figure 2(c)).

Figure 1. (a) Rotting timber sleepers. (b) Sleeper corrosion. (c) Broken sleeper. (d) Sleeper cracking.

As mentioned by You et al. [13] and Kaewunruen et al. [14], laboratory and field tests on mechanical properties are vital for the sustainable development of composite sleepers. Results of laboratory tests, including bending test, electrical resistance test, fatigue test, pull-out test of sleeper screws, and impact load test, confirmed the high performance of FFU sleepers in all aspects [12]. However, the lateral resistance of FFU sleepers with 160 mm in height was as low as wooden sleepers (∼ 9 kN). Sleeper type, size, shape, weight, spacing, and surface texture are the influencing factors on the lateral resistance as well as ballast properties and ballast confinement between sleepers [15–19]. To meet this issue, surface texturing is an efficient method recommended by AREMA standard [10], to increase lateral resistance by 100% in comparison with the typical composite sleeper. In this regard, the construction of bottom-rise sleepers could increase lateral resistance up to 10 kN (Figure 3) [20]. In this regard, ballast components (crib, shoulder, and base) have a significant influence on lateral resistance increment. Results show that the contribution of shoulder ballast, crib ballast, and ballast bed to the lateral resistance of concrete sleepers were about 22.5%, 32.5%, and 37.5%, respectively [21]. In another study, Ferro et al. [22] reported that the number of contacts between composite sleeper and ballast is higher than that of concrete sleeper/ballast interface.

Up to now, there is no investigation on the interaction of sleeper/ballast components as a factor of the lateral resistance of FFU sleepers, as well as the impact of the shoulder height and width on the lateral resistance. In addition, the use of sleeper wings could be another solution to improve lateral stability of composite sleepers which have been already implemented for concrete sleepers [23,24]. In this paper, lateral resistance of different shapes of FFU synthetic sleepers is assessed by a Single Tie Push Test (STPT) to make a comparison between lateral resistance of prototype, winged and bottom-rise FFU sleepers. In the next section, numerical modeling of STPTs is conducted using 3D-laser scanning method and PFC^{3D} to measure the contribution of ballast components to the lateral resistance of FFU sleepers. In the final section, a sensitivity analysis is performed to optimize the dimensions of the textured sleeper.

2. Materials and methods

2.1. Ballast properties
In the present study, basalt aggregates with LAA 18 were used with the particle size distribution according to China National Standard TBT 2140 (Figure 4). It should be mentioned that the bulk density of the ballast layer after compaction was about 1700 kg/m^3.

2.2. Composite sleeper
In this paper, FFU synthetic sleepers produced by KEBOS were used for the tests, which have already been used across China's rail transit system, including conventional railway, urban transit, and heavy haul railway, etc. The FFU sleeper characteristics are shown in Table 1. In this paper, in order to increase
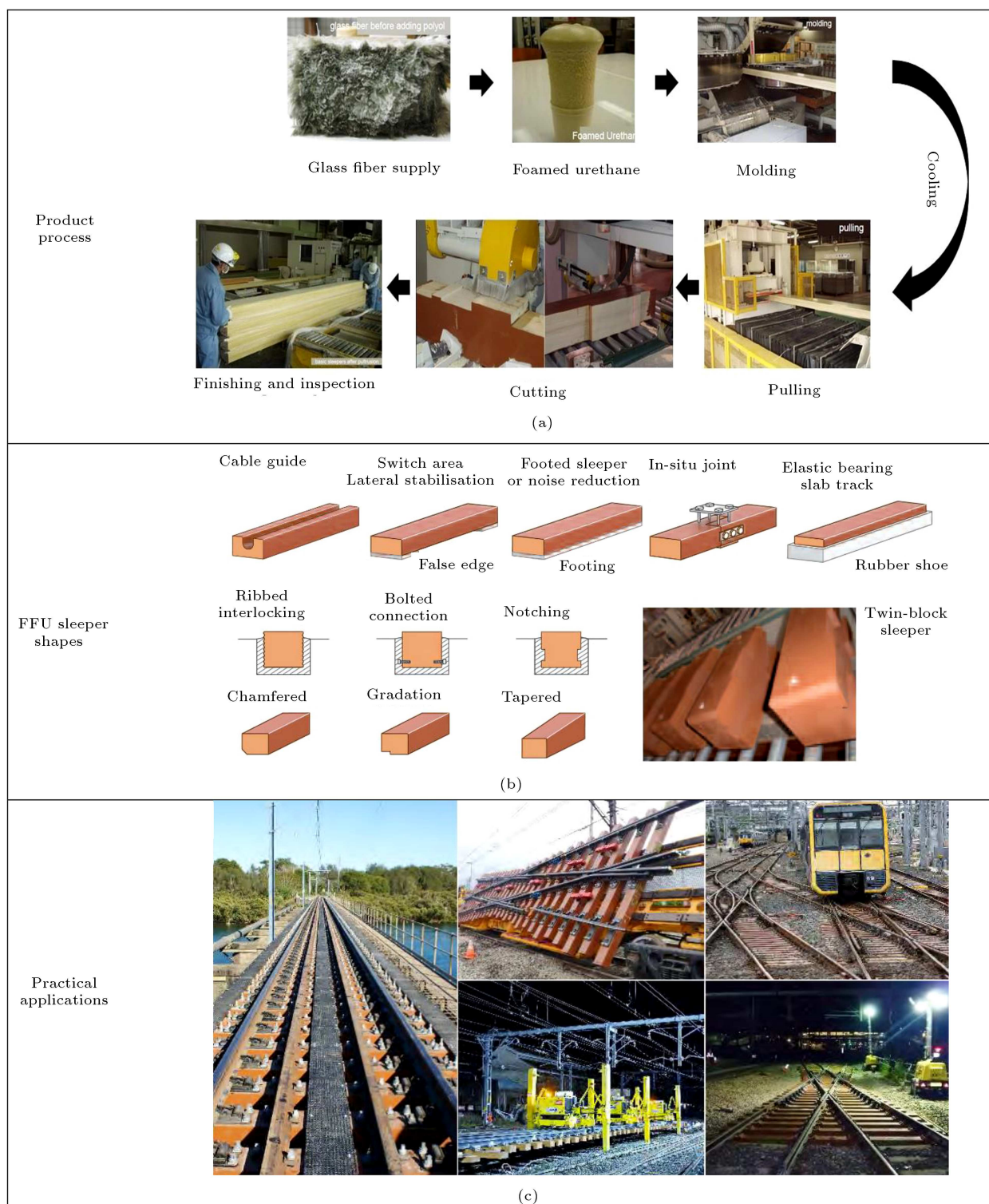
Figure 2. Application of Fiber-reinforced Foamed Urethane (FFU) sleeper on a bridge or ballast track for different functions [12].

the sleeper/ballast interlocking capacity, the optimized types of FFU sleepers were fabricated by adding strip blocks or wings with the same material to the FFU sleeper. In the following, the characteristics of each type are described.

2.2.1. Optimized Type A

Two forms of optimizing the structure are shown in Figure 5(b) and (c). The extruded blocks are set to their outside to increase the disturbing ballast aggregates of the crib ballast. Due to the lower ballast
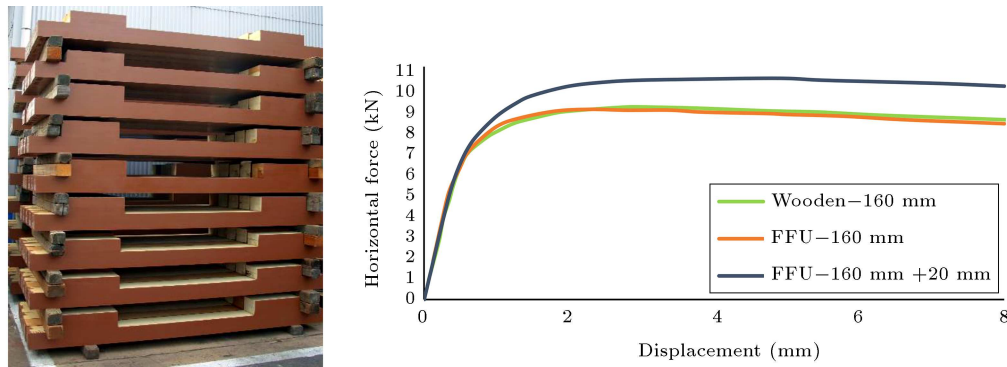
Figure 3. Effect of rising sleeper bottom in rail seats on lateral resistance [20].

Table 1. Fiber-reinforced Foamed Urethane (FFU) synthetic sleeper characteristics [12].

Property		Unit	Beech	FFU synthetic wood				Standard
			New	New	10 years	15 years	30 years	
Density		kg/m^3	750	740	740	740	740	JIS Z 2101
Flexural strength		kN/cm^2	8	14.2	12.5	13.1	11.7	JIS Z 2101
Elastic modulus		kN/cm^2	710	810	800	816	816	JIS Z 2101
Compressive strength		kN/cm^2	4	5.8	6.6	6.3	6.0	JIS Z 2101
Shear strength		kN/cm^2	1.2	1.0	0.95	0.96	0.93	JIS Z 2101
Hardness		kN/cm^2	1.7	2.8	2.5	2.7	2.4	JIS Z 2101
Impact flexural strength	+ 20 C	J/cm^2	20	41	–	–	–	JIS Z 2101
	−20 C	J/cm^2	8	41	–	–	–	JIS Z 2101
Water absorption		mg/cm^2	137	3.3	–	–	–	JIS Z 2101
Insulation resistance	Dry	Ω	$6.6 * 10^7$	$1.6 * 10^{13}$	$2.1 * 10^{12}$	$3.6 * 10^{12}$	$8.2 * 10^{11}$	JIS K 6852
	Wet	Ω	$5.9 * 10^4$	$1.4 * 10^8$	$5.9 * 10^{10}$	$1.9 * 10^9$	–	JIS K 6852
Pull-out force dog rail		kN	25	28	28	23	22	RTRI
Pull-out force screw		kN	43	65	–	–	–	RTRI

confinement between sleepers, there is a low average contact force between crib ballast and sleeper sides. The added blocks are used to increase the confinement pressure to crib aggregates and increase the number of contacts as well. The added blocks are 60 mm × 60 mm × 260 mm in length, width, and height, respectively, and they are made of the same material as FFU.

2.2.2. Optimized Type B
Other forms of FFU sleepers presented in Figure 5(d) and (e), consisted of strip blocks with the dimensions of 10 mm × 10 mm × 240 mm on the sleeper base for type

B1 and strip blocks with the dimensions of 10 mm × 10 mm × 200 mm on lateral sides for type B2, and 100 mm spacing between blocks for the both sleeper types.

2.3. Test method and plan
2.3.1. Test procedure
In this paper, the STPT method was applied to evaluate the lateral resistance of FFU sleepers. Figure 6 shows the instrumentation of the panel for the measurement of lateral force-displacement. Firstly, ballast bed was poured into four layers so that each layer was compressed five times by a vibrating compactor.
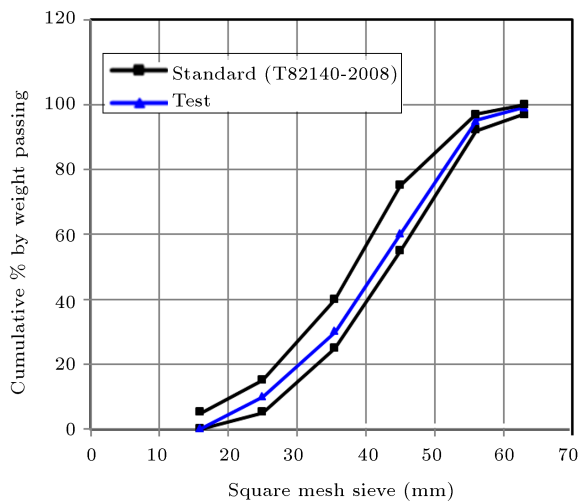
Figure 4. Particle size distribution curve.

Secondly, after placing sleepers, crib ballast was poured into three layers compacted by vibrating compactor. It should be noted that the spacing of the sleepers was 600

mm for all tests. The lateral displacement of sleepers was measured by installation of two Linear Variable Differential Transformers (LVDTs) to the sleeper's end. In order to apply the lateral force, a hydraulic jack with the maximum value of 10 ton loading was fixed by steel rods. In the end, the lateral displacement of the sleeper was equal to the mean of the values obtained from LVDTs. The data logger INV3018A was used to record the lateral resistance force, which was corresponding to 2 mm displacement of the sleeper. The experiment was repeated three times under every test condition, and finally, the average number was considered as sleeper lateral resistance.

2.3.2. Test plan

In order to examine the influence of changes on shoulder height and shoulder width, firstly, STPT tests were performed on different sleepers with a shoulder width of 300, 400, and 500 mm and a shoulder height of 0 and 150 mm, as shown in Table 2. Secondly, since the higher shoulder width led to the higher lateral
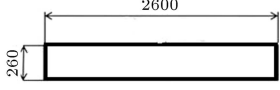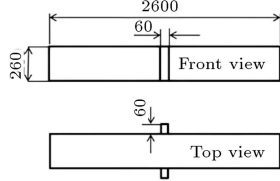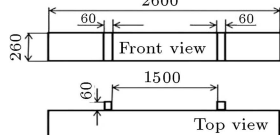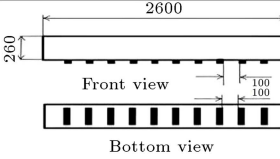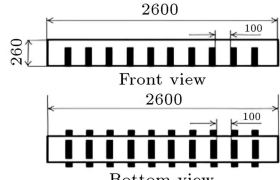

Figure 5. Different shapes of Application of Fiber-reinforced Foamed Urethane (FFU) composite sleepers.
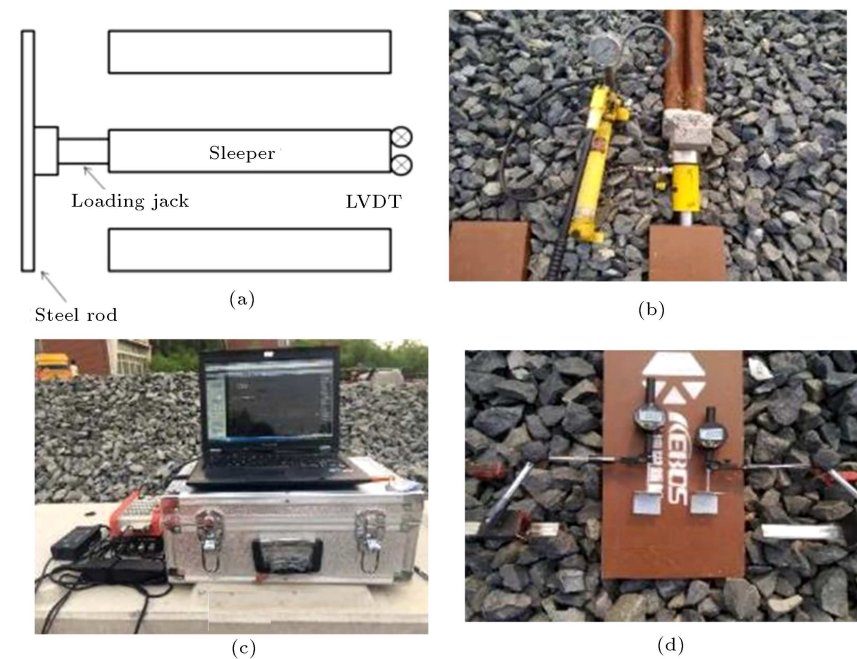
Figure 6. Single Tie Push Tests (STPTs) set up.

Table 2. Test plan for Single Tie Push Test (STPT).

Sleeper type	Shoulder width-shoulder height (mm)					
	300−0	300−150	400−0	400−150	500−0	500−150
Prototype composite	√	√	√	√	√	√
Composite type A1	√	−	−	−	√	√
Composite type A2	√	−	−	−	√	√
Composite type B1	√	−	−	−	√	√
Composite type B2	√	−	−	−	√	√

resistance of ballast, STPTs of 4 types of FFU synthetic sleepers with a shoulder width of 300 and 500 mm, and a shoulder height of 0 and 150 mm was measured.

3. Results and analysis

Figure 7 shows the lateral resistance of sleepers for three sets of sleepers with different test conditions at the horizontal displacement of $d = 2$ mm. In the following, STPTs results are discussed further regarding shoulder height and width variations, as shown in Table 3.

3.1. The influence of shoulder height and width

As depicted in Table 3, along with the growth of shoulder width from 300 to 500 mm and height from 0 to 150 mm, the lateral resistance of both sleepers

Table 3. Shoulder width and height effects on lateral resistance of the prototype sleeper.

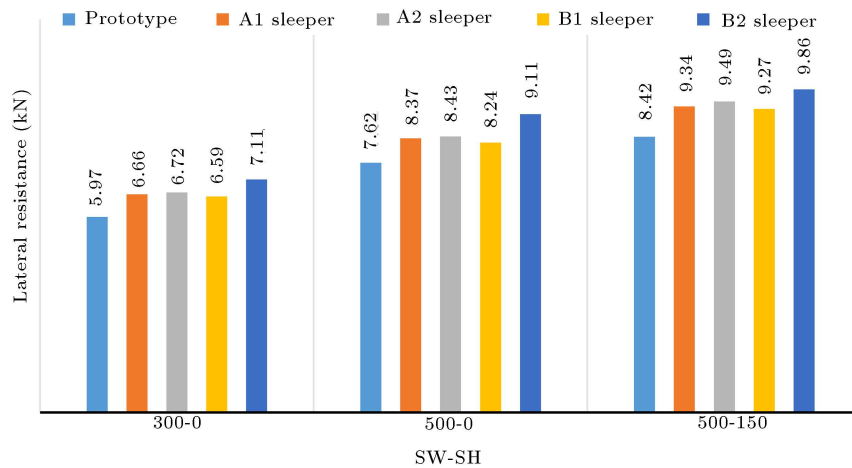| Shoulder width (mm)	Shoulder height (mm)		Impact of shoulder height increment (from 0 to 150 mm)
	0	150	
300	5.97 kN	6.67 kN	11.7%
400	7.06 kN	7.71 kN	9.2%
500	7.62 kN	8.42 kN	10.5%
Impact of shoulder width increment (from 300 to 500 mm)	27.6%	26.2%	−

Figure 7. Lateral resistance of the prototype composite sleeper.

rises. The data of lateral resistance shows an ascending trend throughout the increase in the shoulder width and height so that changes in shoulder width from 300 to 500 mm led to 27.6% lateral resistance increment of the composite sleeper. On the other hand, there was about 10.5% increase in the lateral resistance by rising shoulder height up to 150 mm for panels with a shoulder width of 500 mm. It should be mentioned that the lateral resistance of the concrete sleeper was much higher than the composite one under the same condition, so that the resistance of the concrete sleeper with the shoulder width and height of 500 and 150 mm was about 21.7% higher than that of the prototype composite sleeper.

3.2. Lateral resistance of modified FFU sleepers

As illustrated in Figure 7, with the application of wing-shaped FFU sleepers, types A1 and A2, the lateral resistance compared with the prototype composite sleeper increased. According to the data, sleeper type A2 has a better performance than type A1, but the increment is not significant for the same ballast condition. The lateral resistance of FFU sleepers type B1 and B2 with the strip blocks along sleeper sides and the bottom surface was higher than all types of composite sleepers used in this research. According to the results, sleeper type B2 could increase resistance by an average of 18.5 %. However, no type of composite sleepers can meet the lateral resistance of the concrete sleeper in the same ballast layer condition. In addition, the growth of shoulder width and height lead to an increase in lateral resistance. For instance, the increase of shoulder width of sleepers type A2 and B2 from 300 to 500 mm resulted in 25.4% and 28.1% resistance increment, while the increase of shoulder height from 0 to 150 mm resulted in 12.5% and 8.2% resistance increment, respectively. Therefore, a variation of shoulder width has a higher

impact on the lateral resistance of sleepers which was already proved by previous studies [25,26].

4. DEM simulations of STPT

The Discrete Element Method (DEM) simulation of the STPT was performed using PFC^{3D} and validated with experimental tests in previous studies [24,27]. The impact of the irregular shape of particles on the increase in inter-particle friction angle and the consequential increasing in the lateral resistance of the ballast layer is undeniable [28]. So far, some research has been carried out on simulations of ballast with the real shape [29,30]. Since there is an insignificant difference between the performance of real shape particles and those created by a limited number of overlapped spheres [31–33], the geometry of each particle was filled with 20–25 pebbles. In this regard, 3D images of aggregates were captured to simulate the angularity and surface texture of 3D particles in STPT modeling. In this section, firstly, the DEM modeling of ballast aggregates was performed by 3D scanning method to simulate STPTs. In the next stage, a sensitivity analysis was performed on different shapes of composite sleepers to optimize the sleeper geometry.

4.1. Ballast layer generation

In the first stage, 3D images generated by the laser scanning technique were used to model ballast particles, as shown in Figure 8. In the next stage, the irregular shape of ballast particles was simulated by overlapping a sufficient number of spheres. In order to define the contact between particles, the linear contact model was employed with the allocation of normal and shear contact stiffness (Table 4). It should be noted that the generation of particles was according to the particle size distribution of ballast in experiments. Afterward, wall elements were used to create the geometry of the sleeper in the PFC^{3D} environment.

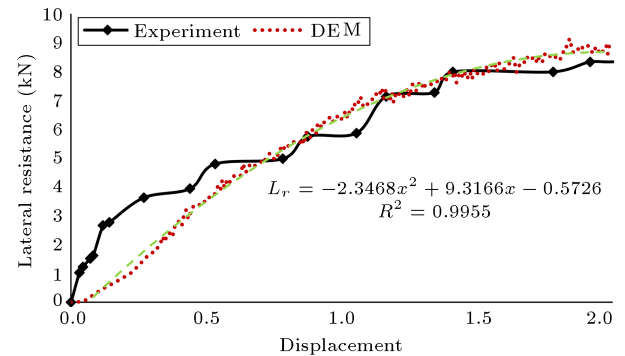**Table 4.** Discrete Element Method (DEM) simulation parameters.

Parameters	Clump	Sleeper (wall)	Wall
Yang's modulus (N/m^2)	2.3e7	–	–
Normal stiffness, k_n (N/m)	6.5e7	1e8	1e8
Shear stiffness, k_s (N/m)	0.75e7	1e8	1e8
Density (kg/m^3)	2700	740	–
Static friction	0.6	0.6	0.6
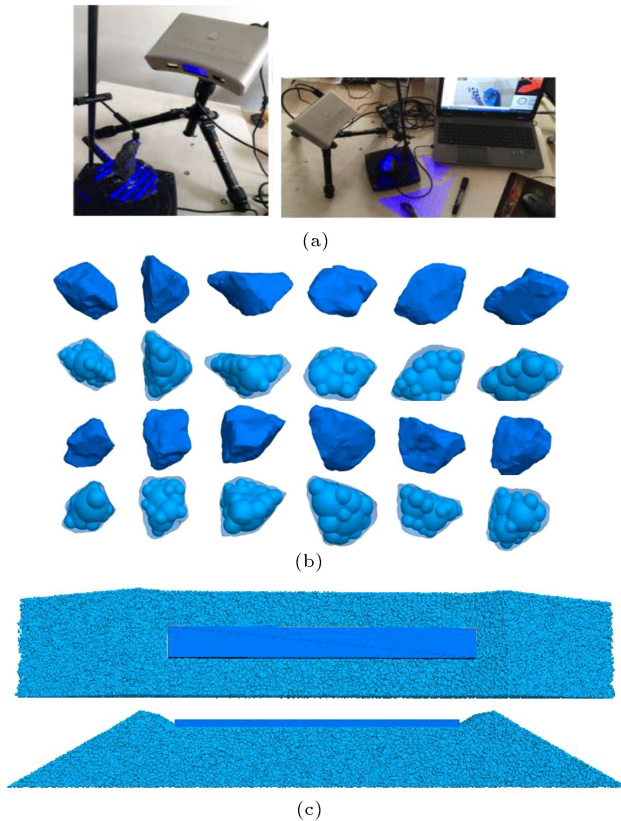
Figure 8. (a) Ballast aggregate 3D scanning. (b) Simulated particles. (c) Simulation of Single Tie Push Test (STPT).

Figure 9. Experimental tests and Discrete Element Method (DEM) simulations of Fiber-reinforced Foamed Urethane (FFU) prototype sleeper.

The weight of the sleeper was applied by the wall servo command, which is the equivalent translation velocity in the z-direction [34]. The final porosity of the ballast layer was 0.32 by using *cycle* command to achieve the equilibrium state. In the end, the contact force between the sleeper and ballast was measured during the displacement of the sleeper with a rate of 1e–5 mm/step.

4.2. Validation of numerical modeling

In order to conduct a sensitivity analysis on the optimization of the FFU prototype sleeper, firstly, the calibration of the numerical model was considered based on the result of the experimental test on a panel with SW_500 and SH_150. As illustrated in Figure 9, the results of numerical modeling is in good agreement with the experimental results so that the difference

between results is about 8.2% at the displacement of 2 mm. The gradual growth of resistance in the initial stage of the DEM simulation might be associated with sleeper sliding along the ballast bed. Since the stability of a DEM model is defined by the *average ratio*, the stability of a model is not the same as the real condition in the final state. Therefore, the steady-state of simulation occurs after more cycles than that of the experiment. According to the force-displacement curve of a simulated sleeper, the lateral resistance of FFU sleeper could be estimated by the following equation:

$$L_r = -2.3468x^2 + 9.3166x - 0.572, \qquad (1)$$

where L_r is lateral resistance and x is the corresponding displacement.

5. Numerical results and discussion

5.1. Contact force distribution

Figure 10 shows the distribution of contact force for FFU sleepers simulated in PFC. It is obvious that the shape of the sleeper is the main feature for changes in sleeper lateral resistance as well as the interaction of the ballast layer and sleeper. For prototype sleepers, due to the smooth surface of sleeper facets, the resistance of the shoulder ballast against sleeper movement is higher than that of ballast bed and crib ballast. This result has a good agreement with those already reported by Ferro et al. [22]. In the case of using side blocks (wings) in sleeper type A2, there is an increase in
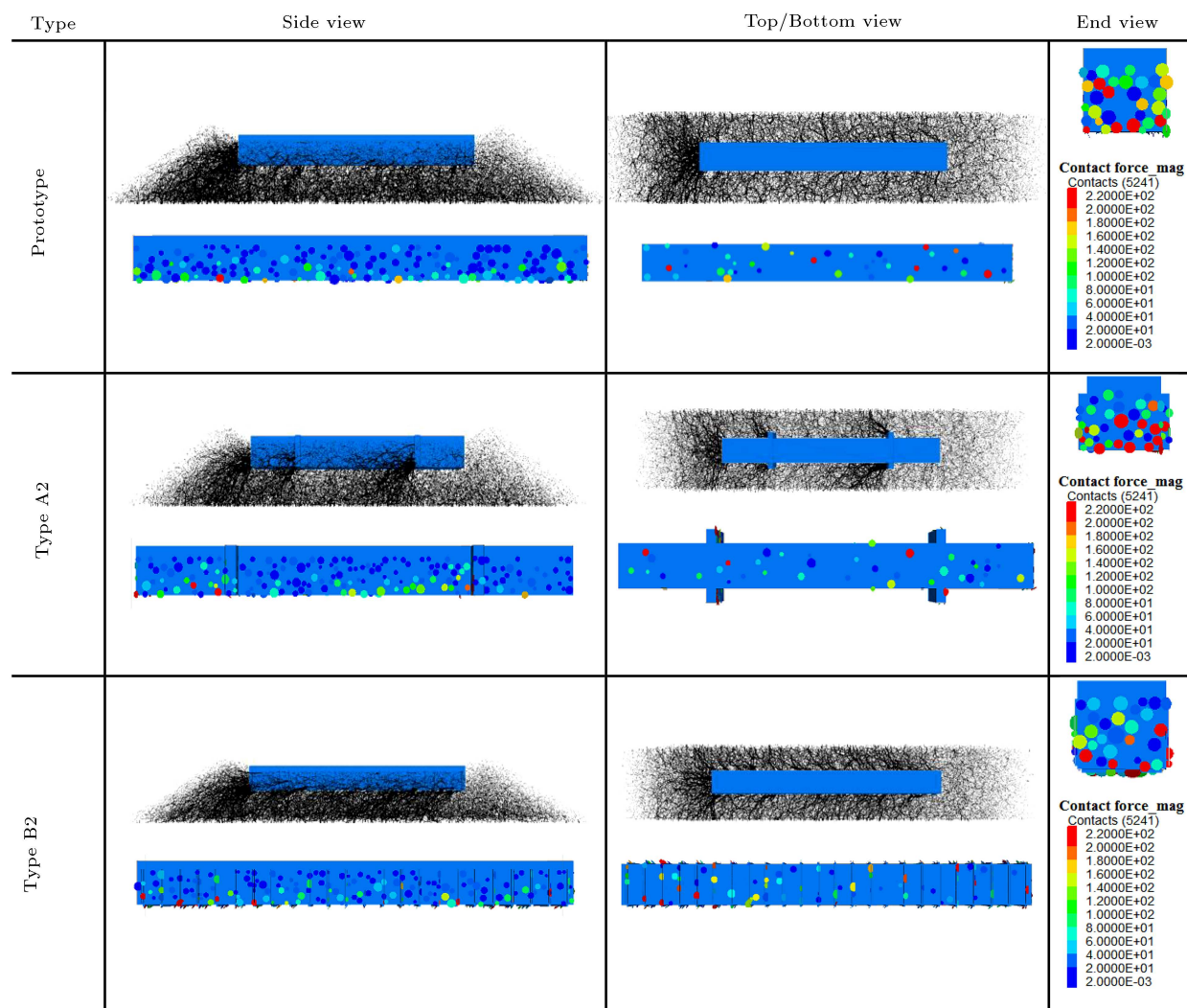
Figure 10. Contact force distribution between ballast particles and sleepers.

the contact force between crib ballast and sleeper sides with non-uniform force distribution through the ballast bed. On the other hand, using strip blocks in the sleeper type B2 lead to increase of force chain uniformly along with the ballast depth as well as crib ballast. Consequently, there is an increase in the contribution of the crib ballast to lateral resistance of sleeper type B2.

5.2. Lateral resistance

In this section, the contribution of the end, bottom, and sides were measured for FFU sleepers with the shoulder height and width of 0 mm and 500 mm, respectively. As illustrated in Figure 11, the resistance of the bottom surface is approximately equal (about 3 kN) for all types of simulated sleepers. This result indicates that the influence of the sleeper bottom surface on resistance increment is insignificant. On the other hand, the smooth surface of the FFU prototype sleeper resulted in less resistance in sleeper sides (19%), while the presence of wings and strip blocks caused

30% and 43% of total resistance for sleepers type A2 and B2. In this regard, due to the continuous bumps of the sleeper type B2, interlocking between sleeper sides and crib ballast increased. Consequently, the side-resistance considerably raised, corresponding to 0.4 mm sleeper displacement. Due to the higher contribution of sleeper sides to the lateral resistance of sleeper type B2, the sleeper end had the lower contribution, while the prototype and sleeper type A2 had almost the same contribution (35%–38%) during the sleeper movement. Overall, the ballast/sleeper interaction led to the higher total resistance of the sleeper type B2 in comparison with other types of sleepers, which was 10 kN, 9.5 kN, and 8.03 kN for sleepers type B2, A2, and prototype, respectively.

5.3. Sensitive analysis

In order to optimize the dimensions of sleeper blocks, a series of sensitivity analyses were performed on the sleeper type A2 with the width of 500 mm and the
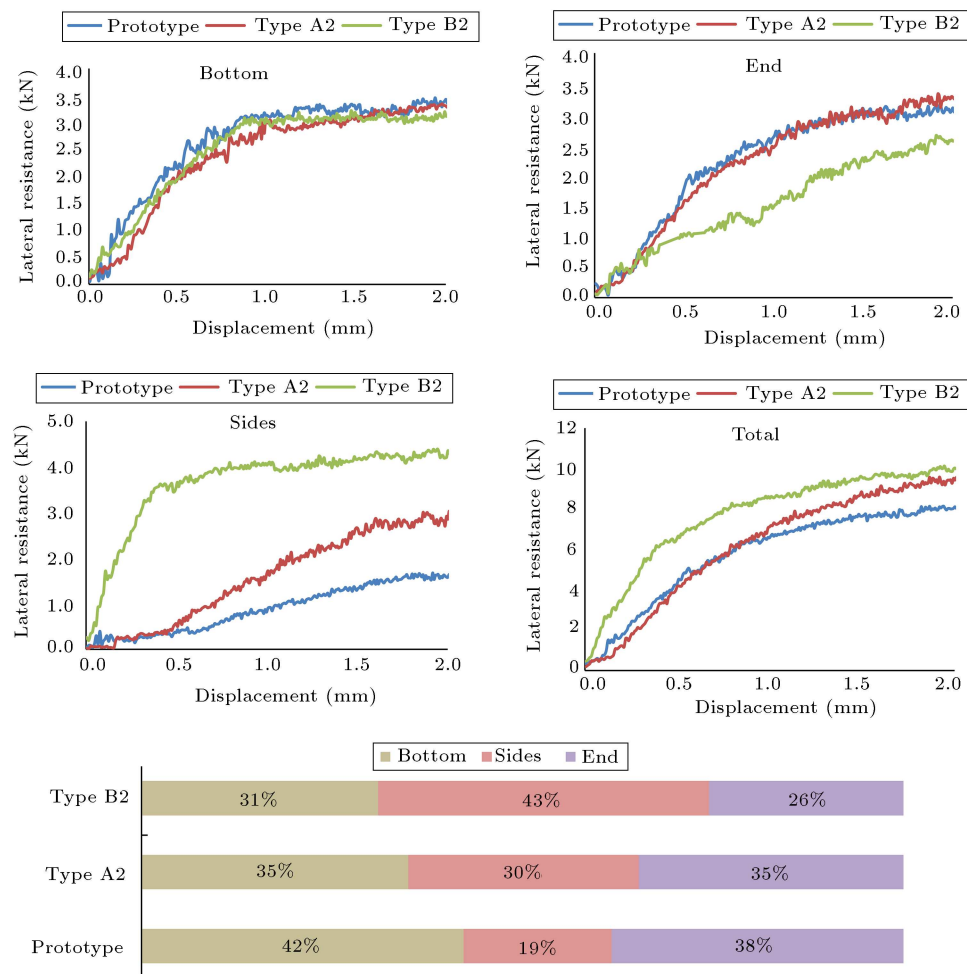
Figure 11. The contribution of sleeper facets to the lateral resistance.

height of 0 mm of a shoulder. In this regard, the numerical analyses were performed on the width of blocks for sleeper type A2 in the range of 6, 8, and 10 cm. It should be noted that the limited sleeper spacing ($S = 60$ cm) leads to practical difficulties in using blocks with a width of higher than 10 cm. Consequently, this value is considered as the maximum width of the sleeper blocks.

As illustrated in Figure 12, the lateral resistance of the sleeper type A2 increased with changes in the width of sleeper blocks from 6 to 10 cm. In general, according to the results and considering the conditions required for the ballast tamping and the slight difference between the lateral resistance of sleepers reinforced by blocks with 8 cm and 10 cm in width, the width of 8 cm can be considered as the optimum size for implementing this type of sleepers in ballasted tracks with regard to railway maintenance and operation practice.

6. Conclusion

Fiber-reinforced Foamed Urethane (FFU) has been recently used in ballasted tracks due to the lower weight
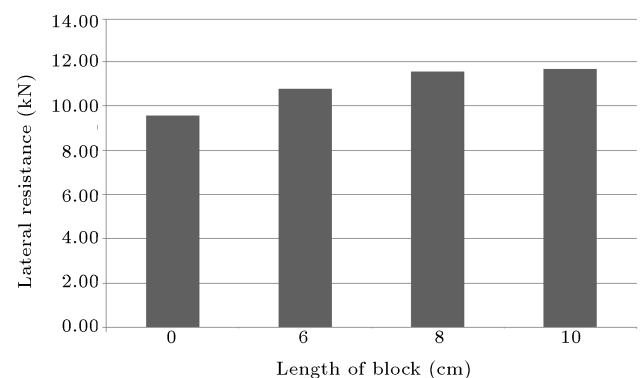
Figure 12. Discrete Element Method (DEM) sensitivity analysis.

and high resistance against vertical loading induced by passing trains. However, it is crucial to study the influence of the low sleeper weight on the lateral resistance of FFU sleepers. Therefore, a series of Single Tie Push Tests (STPTs) were conducted on the ballasted track to investigate the lateral resistance of the prototype FFU synthetic sleeper and its modified types. In the experiments, the shoulder ballast height and width

were investigated as effective factors on the lateral resistance of sleepers. On the other hand, Discrete Element Method (DEM) simulations were performed to determine the contribution of ballast components to the lateral resistance as well as the optimization of the width of wings for the sleeper type A2. The following results can be drawn from this research:

1. The lateral resistance of the prototype FFU synthetic sleeper is 10–15% lower than that of the concrete sleeper;

2. Modified composite sleepers could be applied to increase the lateral resistance. For instance, the resistance increment for composite sleeper type B2 is about 25% in comparison to the prototype;

3. Based on DEM simulations and maintenance operation in railway tracks, blocks with a width of 8 cm could be used for FFU sleepers.

Acknowledgment

References

1. Manalo, A., Aravinthan, T., Karunasena, W., and Ticoalu, A. "A review of alternative materials for replacing existing timber sleepers", *Compos. Struct.*, **92**(3), pp. 603–611 (2010).

2. Ferdous, W. and Manalo, A. "Failures of mainline railway sleepers and suggested remedies-review of current practice", *Eng. Fail. Anal.*, **44**, pp. 17–35 (2014).

3. Sadeghi, J. and Barati, P. "Comparisons of the mechanical properties of timber, steel and concrete sleepers", *Struct. Infrastruct. Eng.*, **8**(12), pp. 1151–1159 (2012).

4. Dogneton, P. "The experimental determination of the axial and lateral track-ballast resistance", In *Railroad Track Mechanics and Technology*, A.D. Kerr, Ed., Pergamon, pp. 171–196 (1978).

5. Profillidis, V., *Railway Management and Engineering*, Routledge (2014).

6. Jing, G. and Aela, P. "Review of the lateral resistance of ballasted tracks", *Proc. Inst. Mech. Eng. Part F J. Rail Rapid Transit*, **234**(8), pp. 807–820 (2020).

7. Ferdous, W., Manalo, A., Van Erp, G., Aravinthan, T., Kaewunruen, S., and Remennikov, A. "Composite railway sleepers-recent developments, challenges and future prospects", *Compos. Struct.*, **134**, pp. 158–168 (2015).

8. Ferdous, W., Manalo, A., and Aravinthan, T. "Bond behaviour of composite sandwich panel and epoxy polymer matrix: Taguchi design of experiments and theoretical predictions", *Constr. Build. Mater.*, **145**, pp. 76–87 (2017).

9. Erp, G. and McKay, M. "Recent Australian developments in fibre composite railway sleepers", *Electron. J. Struct. Eng.*, **13**, pp. 62–66 (2013).

10. AREMA, American Railway Engineering and Maintenance of Way Association, *Engineered Composite Ties*, Part 5, Chapter 30, Man. Railw. Eng., **1** (2012).

11. An-Shuang, L., Delan, Y., and Guoxiang, L. "A study on the application of resin composite sleeper in the design of long-span rail bridges", *Sustain. Transp. Syst., A study on the application of resin composite sleeper in the design of long-span rail bridges*, **2012**, pp. 523–531 (2021).

12. Freudenstein, S. "Investigation on FFU synthetic wood sleeper", Technical University of Munich, Research Report No. 2466, **2008** (2016). https://www.sekisui-rail.com/en/technical-research-on-ffu.html

13. Silva, E.A., Pokropski, D., You, R., and Kaewunruen, S. "Comparison of structural design methods for railway composites and plastic sleepers and bearers", *Australian Journal of Structural Engineering*, **18**(3), pp. 160–177 (2017). https://doi.org/10.1080/13287982.2017.1382045

14. Kaewunruen, S., You, R., and Ishida, M. "Composites for Timber-Replacement Bearers in Railway Switches and Crossings", *Infrastructures*, **2**(4), 13 (2017). https://doi.org/10.3390/infrastructures2040013

15. Montalbán Domingo, L., Real Herraiz, J.I., Zamorano, C., and Real Herraiz, T. "Design of a new high lateral resistance sleeper and performance comparison with conventional sleepers in a curved railway track by means of finite element models", *Lat. Am. J. Solids Struct.*, **11**(7), pp. 1238–1250 (2014).

16. Tanaka, H. and Furukawa, A. "The estimation method of wheel load and lateral force using the axle box acceleration", *Proc. 8th World Congr. Railw. Res.*, Seoul, Korea (2008).

17. Mulhall, C., Balideh, S., Macciotta, R., Hendry, M., Martin, D., and Edwards, T. "Large-scale testing of tie lateral resistance in two ballast materials", *Third Int. Conf. Railw. Technol. Res. Dev. Maintenance, Cagliari*, Sardinia, Italy, pp. 1–12 (2016).

18. Yan-li, Y. "Experimental study on design parameters of longitudinal and lateral resistance of ballast bed for III type concrete sleeper", *J. Railw. Eng. Soc.*, **10**, pp. 49–51 (2010).

19. Indraratna, B., Salim, W., and Rujikiatkamjorn, C. *Advanced Rail Geotechnology-Ballasted Track*, CRC Press (2011).

20. Freudenstein, S. "Lateral displacement resistance of FFU synthetic wood sleepers in consolidated ballasted track", Technical University of Munich, Research Report No. 3484 (2016). https://www.sekisui-rail.com/en/technical-research-on-ffu.html

21. Kish, A., *On the Fundamentals of Track Lateral Resistance*, Am. Railw. Eng. Maint. W. Assoc. (2011).

22. Ferro, E., Harkness, J., and Le Pen, L.J.T.G. "The influence of sleeper material characteristics on railway track behaviour: concrete vs composite sleeper", *Transportation Geotechnics*, **23**, 100348 (2020).

23. Koike, Y., Nakamura, T., Hayano, K., and Momoya, Y. "Numerical method for evaluating the lateral resistance of sleepers in ballasted tracks", *Soils Found.*, **54**(3), pp. 502–514 (2014).

24. Jing, G.Q., Aela, P., Fu, H., and Yin, H. "Numerical and experimental analysis of single tie push tests on different shapes of concrete sleepers in ballasted tracks", *Proc. Inst. Mech. Eng. Part F J. Rail Rapid Transit*, **233**(7), pp. 666–677 (2019).

25. Kabo, E. "A numerical study of the lateral ballast resistance in railway tracks", *Proc. Inst. Mech. Eng. Part F-journal Rail Rapid Transit-Proc Inst Mech Eng F-J Rail R*, **220**, pp. 425–433 (2006).

26. Le Pen, L.M. and Powrie, W. "Contribution of base, crib, and shoulder ballast to the lateral sliding resistance of railway track: a geotechnical perspective", *Proc. Inst. Mech. Eng. Part F J. Rail Rapid Transit*, **225**(2), pp. 113–128 (2010).

27. Jing, G., Fu, H., and Aela, P. "Lateral displacement of different types of steel sleepers on ballasted track", *Constr. Build. Mater.*, **186**, pp. 1268–1275 (2018).

28. Laryea, S., Baghsorkhi, M.S., Ferellec, J.F., McDowell, G.R., and Chen, C. "Comparison of performance of concrete and steel sleepers using experimental and discrete element methods", *Transp. Geotech.*, **1**(4), pp. 225–240 (2014).

29. Khatibi, F., Esmaeili, M., and Mohammadzadeh, S. "DEM analysis of railway track lateral resistance", *Soils Found.*, **57**(4), pp. 587–602 (2017).

30. Ferellec, J.-F. and McDowell, G.R. "A method to model realistic particle shape and inertia in DEM", *Granul. Matter*, **12**(5), pp. 459–467 (2010).

31. Xu, Y., Gao, L., Zhang, Y., Yin, H., and Cai, X. "Discrete element method analysis of lateral resistance of fouled ballast bed", *J. Cent. South Univ.*, **23**(9), pp. 2373–2381 (2016).

32. Guo, Y., Zhao, C., Markine, V., Jing, G., and Zhai, W. "Calibration for discrete element modelling of railway ballast: A review", *Transp. Geotech.*, p. 100341 (2020).

33. Zhang, D., Huang, X., and Zhao, Y. "Investigation of the shape, size, angularity and surface texture properties of coarse aggregates", *Constr. Build. Mater.*, **34**, pp. 330–336 (2012).

34. Itasca, M., *Particle Flow Code in Three Dimensions (PFC3D)*, Minneapolis (2008).

Biographies

Guoqing Jing has research interests in testing and modeling of ballasted track, i.e., (1) sleeper ballast aggregates interactions, 3D characterization of ballast using imaging techniques, as well as GPR in the railway system; (2) recycled material for modern ballasted track and innovative structure, i.e., composite sleeper, under sleeper pad or hybrid sleeper, analyses of recycled materials into ballasted track such as tire rubber, asphalt, glass, fiber into the concrete sleeper, and even modern steel sleeper; (3) modeling of ballast using discrete and finite element methods and mechanistic-based design; (4) ballast flight of HSR and ballast tamping maintenance. Dr. Jing has served as an investigator on over 20 research projects with grants received from NSFC, CRC, CREC, CRCC, CCCC government, and railway-related industry. He is invited as chief consultant for Mexico, Iran, Russia HSR, and Tanzania railway projects.

Lu Zong received the BS degree in Civil Engineering from Lanzhou Jiaotong University in 2017. She is currently studying for MS degree in Highway and Railway Engineering from Beijing Jiaotong University. Her main research is railway ballasted track.

Yameng Ji received a BS degree in Civil Engineering from Shijiazhuang Tiedao University in 2017 and an MS degree in Highway and Railway Engineering from Beijing Jiaotong University in 2020. In her undergraduate period, her main research was on railway ballasted track. She is currently studying for Doctoral degree in Civil Engineering at the University of Nantes, France. Her research focuses on building materials of 3D printing and application to the construction of the structural walls of buildings.

Peyman Aela has been a PhD candidate at the Department of Civil Engineering at Beijing Jiaotong University since 2017. After graduating with a BEng (Civil Engineering) from the Isfahan University of Technology, Iran, in 2014, he was trained as a railway engineer and received an MS degree from Iran University of Science and Technology in 2017. His main research expertise lies in modeling the ballast railway tracks using the Discrete Element Method (DEM) and has published 10 SCI papers in the field of lateral track stability.